Characterization of the X-ray eye

Report by Willem Rischau
Friedrich Schiller University Jena, Germany
DESY Summer School 2009

21.07.2009 - 10.09.2009

1 Introduction

Detectors for X-ray imaging can be realised in different ways, depending on the energy range, the requested spatial resolution and detective quantum efficiency. One way to realise an X-ray detector with a spatial resolution in the micrometer range is the combination of a single crystal scintillator, a light microscopy optics and a charged-coupled device (CCD). This work is about the characterization of such an X-ray camera or X-ray eye, whose setup is based on plans from *M. Bordessoule* at the *SOLEI Synchrotron* [4]. This camera will be part of the detector loan pool at HASYLAB and should be used later at *PETRA III* beamlines to find the synchrotron beam. Therefore, it should be fast and adaptable to different energies and resolutions. In this work, the spatial resolution of the optical system consisting only of the CCD camera and the microscopy objective was determined as well as the spatial resolution of the complete X-ray eye with installed scintillator screen.

2 X-ray detectors

2.1 Principles of X-ray detection

The detection of X-rays is based in principle upon the creation of electron-hole pairs in a semiconductor or an electron-ion pair in a gas through different light-matter interactions like the photoelectric or the Compton effect. This can be realised in a detector in two different ways, either in indirect or direct detection. In indirect detection the X-ray photons are first converted into visible light photons by using a scintillator screen which then generate a signal in the sensor, whereas in direct detection the X-ray photons are directly converted into an electric signal by creating electron-hole pairs. The advantage of the indirect detection is the possibility to use commercial CCD cameras for the detection of the created visible photons whereas

direct detection can only be realised with X-ray sensitive cameras.
The X-ray detector described and investigated in this work is based on indirect detection and basically consists of a scintillator screen, a light microscopy optics and a CCD Camera. With this design, a spatial resolution in the micrometer range can be achieved. The schematic setup of this kind of x-ray camera is shown in figure

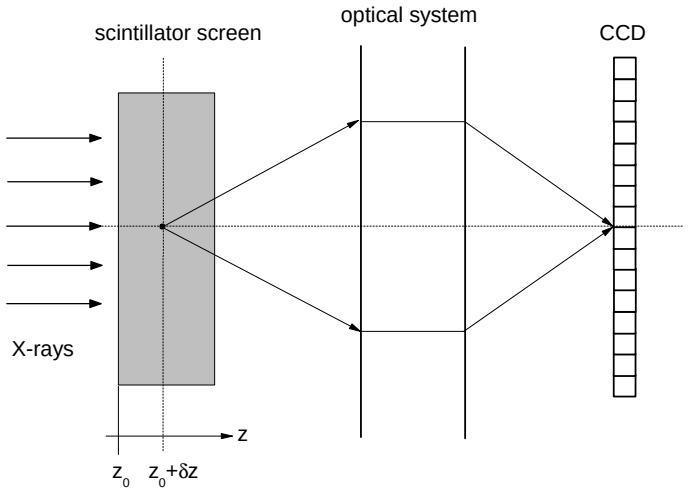

Figure 1: Schematic setup of an X-ray camera consisting of a scintillator screen, a microscopy optics and a CCD camera.

1. The incoming X-ray photons create identical visible-light images in the different planes of the scintillator screen. If the CCD camera is focused on the plane at the position z_0 of the scintillator screen, all planes at the position $z_0 + \delta z$ are out of focus at the CCD. Therefore, the spatial resolution of the camera decreases with increasing scintillator thickness. As the absorption of X-ray photons and therefore also the efficiency decreases with thinner scintillator thicknesses, one always has to find a compromise between spatial resolution and detector efficiency.

2.2 Determination of the spatial resolution

The spatial resolution of an optical system, like a camera can be described by his impulse response to different sources. In the case of a point source or a point object, the response of the system is called point spread function (PSF). If an optical system is considered as a linear system, the image of two objects is given by the linear superposition of two independent images corresponding to the two objects.

Therefore, each image point can be considered as the weighted sum of the point spread functions corresponding to each point $\mathbf{u}$ in the object plane. Mathematically, the object signal can be expressed as a weighted sum over 2D delta-impulses:

$$w_{in}(\mathbf{u}) = \int w_{in}(\mathbf{u'})\delta(\mathbf{u} - \mathbf{u'})d\mathbf{u'} \tag{1}$$

with an impulse $\delta(\mathbf{u}-\mathbf{u'})$ at the point $\mathbf{u}$ in the object plane and a weighing function $w_{in}(\mathbf{u})$ depending on the object. The output signal and the image itself, respectively can then be described as

$$w_{out}(\mathbf{u}_0) = \int w_{in}(\mathbf{u})PSF(\mathbf{u}_0, \mathbf{u})d\mathbf{u}, \tag{2}$$

where $w_{out}(\mathbf{u}_0)$ is the output signal at the spatial position $\mathbf{u}_0$ in the image plane and $\mathrm{PSF}(\mathbf{u}_0, \mathbf{u})$ is the response of the system measured at point $\mathbf{u}_0$ to an impulse $\delta(\mathbf{u} - \mathbf{u'})$ applied at $\mathbf{u}$.

If the point spread function $\mathrm{PSF}(\mathbf{u}_0, \mathbf{u})$ is independent of the position $\mathbf{u}$ in the object plane, the system is called shift invariant. Often, the PSF of a linear system only depends of the difference of its two arguments. In case of an optic system, this is true if the image of a point source does not depend on the location of the point. In this case eq. (2) becomes a convolution or folding integral:

$$w_{out}(\mathbf{u}_0) = \int w_{in}(\mathbf{u})PSF(\mathbf{u}_0 - \mathbf{u})d\mathbf{u}. \tag{3}$$

As the experimental realization of a point source is very difficult, it is more convenient to measure the line spread function (LSF) or the edge spread function (ESF) of a system. While the LSF is the response of the system to a line source, the ESF expresses the systems response to a sharp edge, see figure 2. The spatial resolution of the system can be expressed by the width of the LSF or the ESF, i.e. the Full-Width-at-Half-Maximum (FWHM) of the LSF or sometimes the 10%-to-90% distance of the edge response. The advantage of the ESF is the easy experimental realization of an edge. As the two-dimensional derivative of an edge is a line, the LSF can be determined by deriving the edge response. Moreover, as a line source can be regarded as the integral of a point source, the one-dimensional derivative of the ESF in a certain direction is the PSF. Therefore, the spatial resolution of the system can be expressed by the FWHM of the PSF, derived from the measured ESF of the system.

Another way to express the spatial resolution of an imaging system is the Modulation Transfer Function (MTF). The MTF is defined as the the ratio of the output modulation M_{out} of the signal measured by the detector to the input modulation M_{in} of the signal. This corresponds to the Fourier transform of the one-dimensional PSF (or alternatively the Fourier transform of the two-dimensional LSF):

$$MTF = \frac{M_{out}}{M_{in}} = |FT\{PSF\}| \tag{4}$$

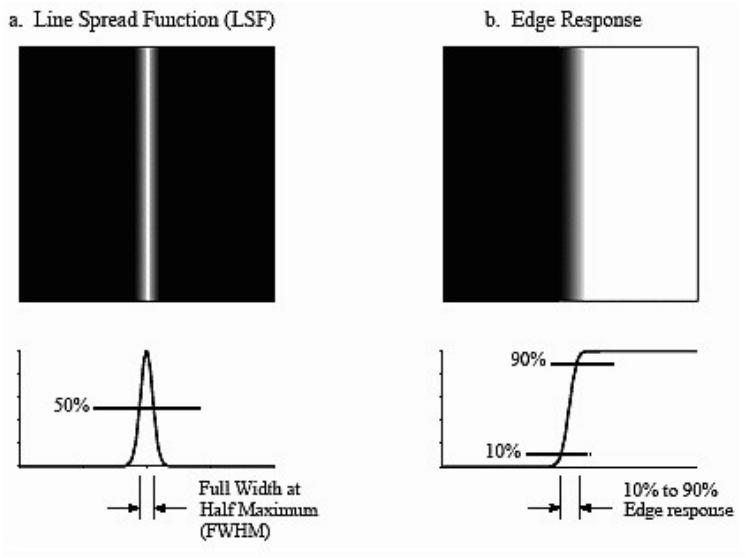

Figure 2: Line spread function (LSF) and edge spread function (ESF). While the width of the LSF is expressed by the FWHM, the width of the ESF is usually expressed as 10%-to-90% distance of the edge response[3].

The modulation or contrast of a signal is defined by

$$M = \frac{w_{max} - w_{min}}{w_{max} + w_{min}} \tag{5}$$

with the maximum and minimum amplitude w_{max} and w_{min}, respectively. As the Fourier transform of an even function is again an even function, a symmetric PSF results in a symmetric MTF. This applies for example in the case of a Gaussian distributed PSF

$$PSF(x) = \exp\left[-\frac{1}{2}\left(\frac{x}{\sigma}\right)^2\right] \qquad \Rightarrow \qquad MTF(k) = \exp\left[-\frac{1}{2}(k\sigma)^2\right] \tag{6}$$

with the spatial position x in the image plane, the wavevektor k and a standard deviation σ of the distribution. The MTF corresponds to the frequency response of the system, i.e. it indicates the response amplitude of the system as a function of the spatial frequency. The spatial resolution is then usually expressed as the frequency where the MTF is reduced to 10%.
The spatial resolution can though be expressed in several ways, which provide different values. The FWHM of the PSF and the 10% value of the MTF do not correspond to the same value for the spatial resolution.

3 Experimental Setup

3.1 X-ray eye

The used X-ray eye (see figure 3) was constructed according to plans from *M. Bordessoule* at the *SOLEI Synchrotron* [4]. The camera uses a 45° mirror, so the incoming X-rays form a 90° angle with the optical axis of the microscopy optics and the CCD. The CCD camera used for the measurements on the following pages is a *Prosilica GC 650* with a pixel size of $9.9 \times 9.9 \mu m^2$ whereas the camera setup shown in figure 3 uses the *Basler Scout SCA640-74gm Gigabit Ethernet* camera, which was used for some first tests until the Prosilica camera was available (for further explanation see chapter 5). The used objective is a *Computar M5018-MP2* Megapixel Lens with a magnification of 1.8 and a 50mm focal length. For more information on the different parts and the camera itself, see [4]. The scintillator screen is a yttrium

Figure 3: X-ray camera with a *Basler Scout SCA640-74gm Gigabit Ethernet* camera.

aluminium garnet $Y_3Al_5O_{12}$ (YAG) single crystal. Figure 4 shows the absorption coefficient of YAG for the two used scintillator thicknesses 100 and $200 \mu m$.

3.2 Measurement of the spatial resolution

To determine the spatial resolution of the optical system, consisting out of the microscope objective and the CCD camera, the point spread function was measured by illuminating a sharp edge with a red LED. In order to move the LED very close to the edge, the originally round head of the LED was filed down to a plane shape. The edge itself was realised with a thin piece of tantal foil with a polished edge, which was then glued to a microscopy cover glass. The prepared cover glass was then installed in the camera in the focus of the camera, i.e. in the position of the scintillator screen. The LED could be moved using a micrometer translation device. After a picture with the edge, the LED was moved and the cover glass with the glued edge was removed and exchanged for a normal cover glass. After this, the LED was moved back in the starting position and a second picture was taken under

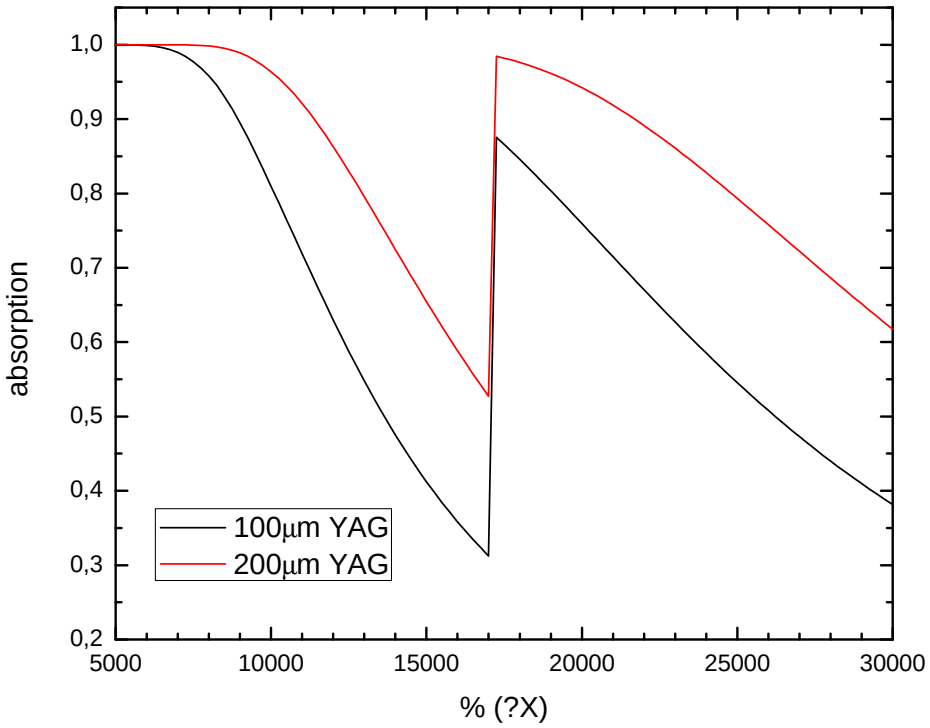

Figure 4: Absorption coefficient of yttrium aluminum garnet $Y_3Al_5O_{12}$ (YAG) for a crystal thickness of 100 and 200μm.

the same conditions. This picture was used to determine the flat field to account the different sensitivity of the pixel as well as the influence of the source. Another picture was taken with the closed lens cap to determine the dark current. Each image was therefore normalized, i.e. first the dark current was subtracted from the image (with edge) and the flat field image (without edge) and then the image itself was divided by the flat field image.

The spatial resolution of the complete X-ray eye was measured in a similar way with X-rays using a fine focus X-ray tube with Mo target (anode voltage $U = 30keV$) and a collimator system so that the effective source size is small compared to the spatial resolution. This time, the edge was fixed on the scintillator screen.

The CCD camera was used with the *Prosilica Sample Viewer*, the evaluation of the pictures was done with an IDL software written by *Michael Lohmann*.

4 Measurements

4.1 Spatial resolution of the optical system

The spatial resolution of the optical system of the x-ray eye was measured with a CCD exposure time of 3s and a LED illumination period of 8ms. Figure 5 shows the taken pictures with and without the edge. The corresponding edge spread function,

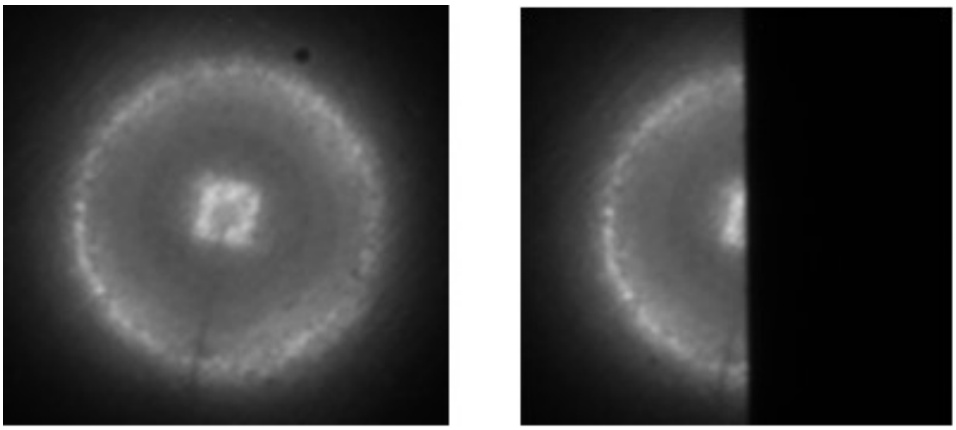

Figure 5: Images of the LED without (left) and with (right) the edge for an CCD exposure time of 3s and a LED illumination peroid of 8ms.

the point spread function (one dimensional line spread function) and the modulation transfer function are shown in figures 6 and 7, respectively. A spline interpolation calculate points at 10nm distances from the measured ESF, the PSF was derived from the interpolated ESF and finally a Gauss function (see eq. 6) was fitted on the PSF. The determined spatial resolution, corresponding to the frequency where the MTF is reduced to 10% is 55 lines per millimeter corresponding to $18\mu m$.

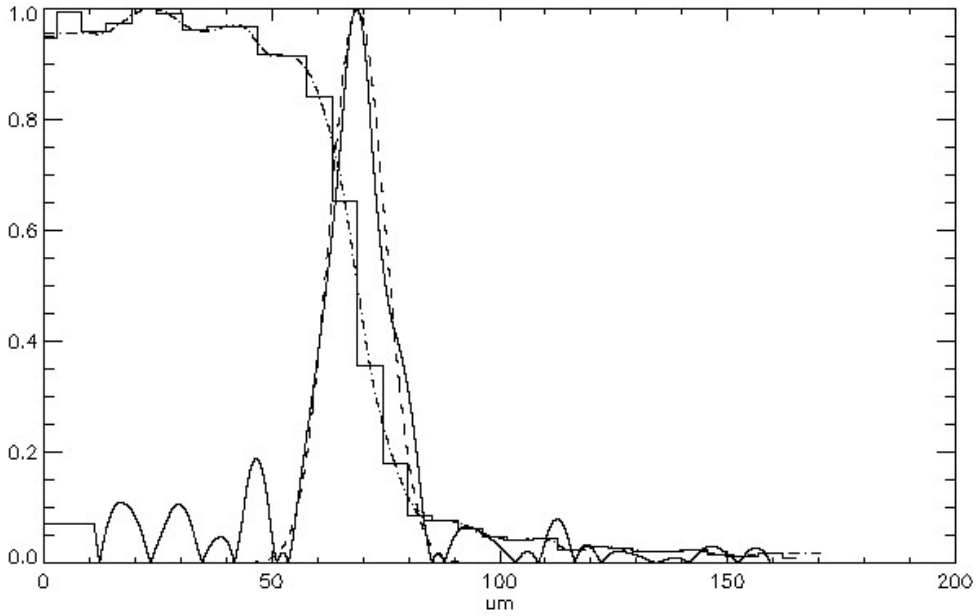

Figure 6: Measured and fitted (dashed-dot line) ESF, derived PSF and fitted Gaussian distribution (dashed line).

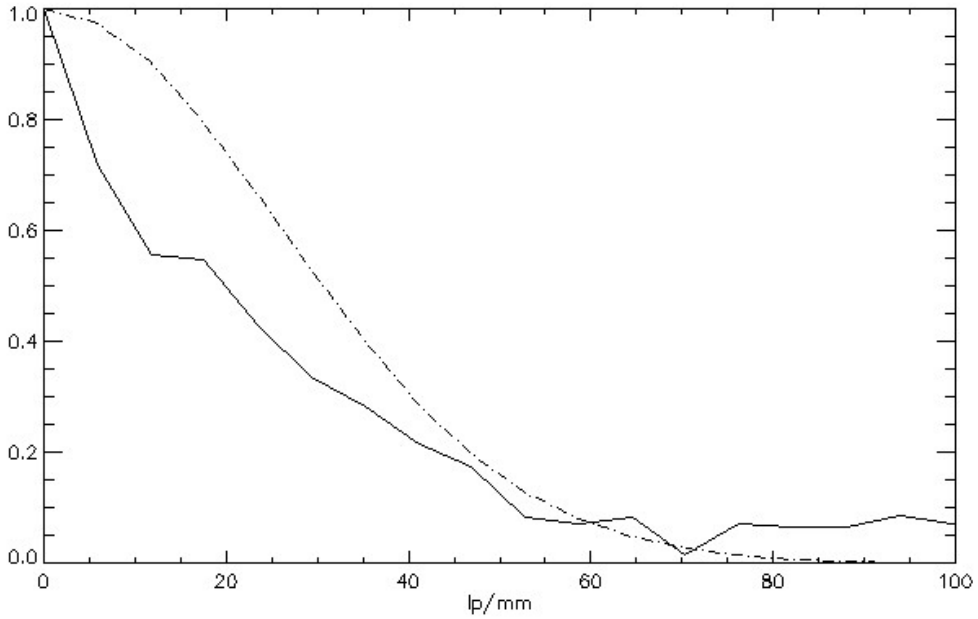

Figure 7: MTF, derived from the fit of the PSF and the Gaussian distribution shown above in figure 6.

4.2 Spatial resolution of the X-ray eye

Figure 8 shows the measured and fitted PSFs and MTFs respectively for the 100 and the 200μm scintillator. The results for the spatial resolution of the complete X-ray determined from these figure as well as the spatial resolution of the optical system are given in table 1.

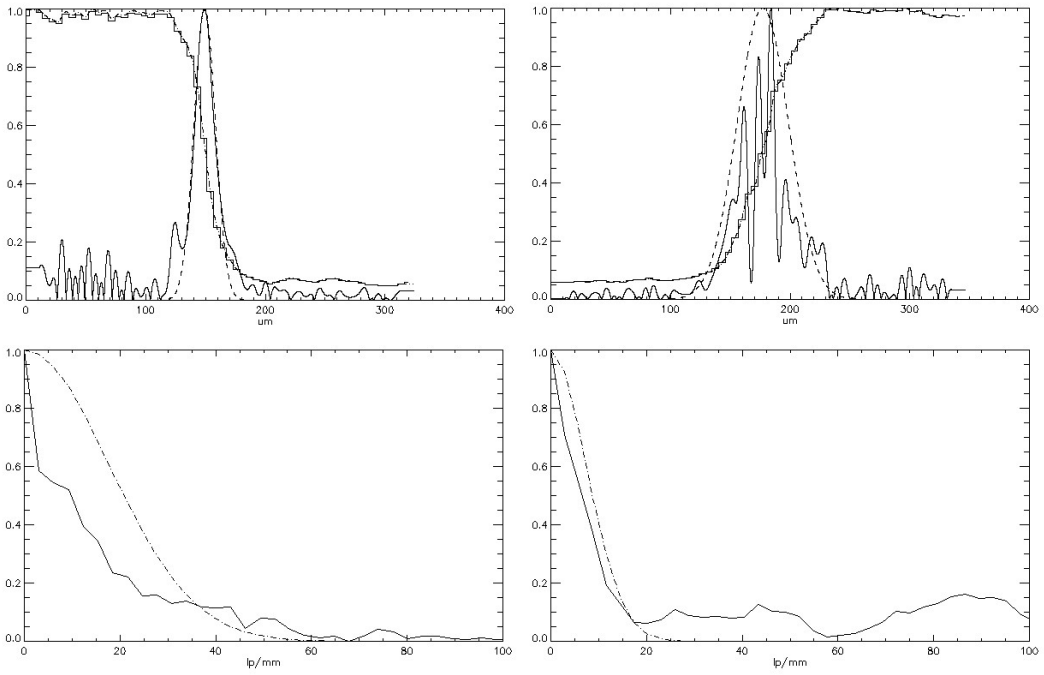

Figure 8: **Top:** Measured and fitted (dashed-dot line) ESF and the derived PSF and fitted Gaussian distribution (dashed line) for the 100μm **left** and the 200μm **right** single crystal scintillator for a CCD exposure time of 60s to the X-rays. **Bottom:** Corresponding MTFs. The shown ESF curves are smoothed by factor 2.

System	FWHM of the PSF [μm]	10 % of MTF [lp/mm]	10 % of MTF [μm]
optical system	14	55	18
100μm YAG	21	41	24
200μm YAG	51	16	63

Table 1: Spatial resolutions of the optical system of the X-ray eye and of the complete X-ray eye with the 100 and the 200μm YAG scintillator screen.

5 Summary

In this work, I characterized an X-ray eye, which should be used as a beamfinder at *PETRA III* beamlines. This included the determination of the spatial resolution of the optical system, consisting of a CCD camera and a microscopy optics as well as the spatial resolution of the complete X-ray eye with installed scintillator screen. This was done by measuring the systems response to a sharp edge, illuminated with a LED and X-rays, respectively. The result for the spatial resolution corresponds to the 10% value of the modulation transfer function, which was obtained by deriving the measured point spread function. The result for the optical system is lying in the range of $20\mu m$, which is larger than the expected resolution for this setup. This could be due to the use of the LED, i.e. a too inhomogenous light source or a not accurate enough focus of the camera on the used edge. The spatial resolution for the complete X-ray eye is in the range of 20 and $60\mu m$ for a 100 and $200\mu m$ YAG scintillator screen, respectively

All results in this work were obtained with the *Prosilica GC 650* camera. At the beginning of this work, only the colour version of this camera was available. Tests with this version showed however, that it is not possible to obtain raw uninterpolated data from each pixel. This made it impossible to use the colour version for the determination of the spatial resolution, as the expected resolution lies in the same range as the pixel size. The spatial resolution of the optical system was also determined with another CCD camera, the *Basler SCA640-gm*. Both cameras have similar features, but the LINUX drivers of the *Basler* camera do not work with the *LINUX* version at *DESY* and it is impossible to obtain images with more than 8bit using the Basler software *Pylon Viewer*.

6 Acknowledgements

First, I would like to thank DESY for allowing me to get an insight into the life at a big research facility. Special thanks goes to my supervisor Michael Lohmann for his help, anytime I needed it.

References

[1] T. Martin, A. Koch: *Recent developments in X-ray imaging with micrometer spatial resolution*, J. Synchrotron Rad. (2006) 13 180-194

[2] H.H. Barrett, W. Swindell *Radiological imaging: the theory of image formation, detection, and processing, Volume 1* Academic press of the university of Michigan (1981)

[3] S.W. Smith: *The Scientist and Engineer's Guide to Digital Signal Processing*, www.dspguide.com.

[4] M. Bordessoule: *Caméra à grandissement 1 pour ODE. Caméra à 90° du faisceau X*, (2007)